

## Stability and thermophysical properties enhancement of Al<sub>2</sub>O<sub>3</sub>-water nanofluid using cationic CTAB surfactant

Bhavin Mehta<sup>a,\*</sup>, Dattatraya Subhedar<sup>a</sup>, Hitesh Panchal<sup>b</sup>, Kishor Kumar Sadasivuni<sup>c,\*</sup>

<sup>a</sup> Chamos Matrusanatha Department of Mechanical Engineering, Chandubhai S. Patel Institute of Technology Charotar University of Science & Technology, Changa, Dist. Anand, Gujarat, India

<sup>b</sup> Department of Mechanical Engineering, Government Engineering College, Patan, Gujarat, India

<sup>c</sup> Centre for Advanced Materials, Qatar university, Qatar & Department of Mechanical and Industrial Engineering, Qatar University, PO Box 2713, Doha, Qatar

### ARTICLE INFO

#### Keywords:

Nanofluid  
Long-term stability  
Synthesis  
Sonication  
Surfactant  
Thermal conductivity  
Viscosity

### ABSTRACT

Excellent thermal characteristics of homogeneous dispersion of nano-sized particles in a carrier fluid (nanofluid) make it appealing for use in a variety of thermal applications. The study aims to prepare stable aqua-Al<sub>2</sub>O<sub>3</sub> nanofluid utilizing a two-step method. To increase nanofluid stability, a cationic surfactant called cetyltrimethylammonium bromide (CTAB) is used. The carrier fluid is heated while magnetic stirring is used to increase nanoparticle distribution. Bath sonication with concurrent heating and probe sonication is used to improve long-term stability. The chemical composition of  $\gamma$ -Al<sub>2</sub>O<sub>3</sub> was confirmed by X-ray diffraction (XRD) results, and Scanning Electron Microscopy (SEM) images revealed the shape and mean size of the particles. The stability of the synthesized sample is evaluated utilizing a variety of stability evaluation techniques, including visual examination, UV-vis spectrometry, and Dynamic Light Scattering (DLS), at various time intervals, including 1, 8, 15, and 30 days. After 15 days of manufacture, the stability of the nanofluid without surfactant was low. Due to improved particle suspension, nanofluid with surfactant has demonstrated greater UV-vis light absorption. After a month of synthesis, it was discovered that the mean particle sizes of suspended nanoparticles in carrier fluid were 80 nm and 536 nm for nanofluid with and without surfactant respectively. KD2Pro thermal analyzer and viscometer were used to measure the thermal conductivity and viscosity of nanofluid. As per the experimental results, a nanofluid's thermophysical characteristics were found to be improved with volume concentration of nanofluid. Maximum augmentation in thermal conductivity and dynamic viscosity is 8.5% and 76.2% respectively at 1% nanofluid volume concentration.

### 1. Introduction

Nanofluid consists of homogeneous suspensions of nano-sized particles in a carrier fluid. It has gained significant attention in recent years for its potential use in thermal applications. The use of nanofluids as a heat transfer fluid has shown promise because of their attractive thermal properties and increased thermal conductivity compared to traditional fluids [1]. Nano-sized particles consist of a high surface area to volume ratio resulting in augmentation of heat transfer amongst particles and a carrier fluid [2]. The increased thermal conductivity can enhance the heat transfer performance of the fluid, leading to enhanced heat transfer rates and reduced energy consumption. Additionally, the size and shape of nanoparticles can be tailored to optimize their thermal properties for specific applications [3]. For example, carbon nanotubes are

particularly effective in improving heat transfer performance in some applications. However, there are also challenges associated with the usage of nanofluids in several thermal appliances. The stability of the nano-sized particles in the carrier fluid is a major concern, as they may agglomerate or settle over time, reducing the effectiveness of the nanofluid. Furthermore, the production cost of nanofluids is usually greater than conventional working fluids, and their long-term durability and environmental impact are still under investigation [4]. As a result, the appropriateness of using nanofluids for certain thermal applications must be determined on a case-by-case basis, taking into account the application's unique requirements as well as the potential advantages and disadvantages of doing so.

Nanofluids are typically synthesized by dispersing nanoparticles into a base fluid, using a variety of methods. The choice of method is subject

\* Corresponding authors.

E-mail addresses: [bhavinmehta.me@charusat.ac.in](mailto:bhavinmehta.me@charusat.ac.in) (B. Mehta), [kishorkumars@qu.edu.qa](mailto:kishorkumars@qu.edu.qa) (K.K. Sadasivuni).

to several influencing parameters, for instance, particle material, carrier fluid type, and the desired properties of the resulting nano-synthesized fluid. Some of the commonly used methods for synthesizing nanofluids are one-step method and two-step method. In one-step method, nano-sized particles are synthesized directly in the carrier fluid. For example, metal nanoparticles can be synthesized in a liquid medium using chemical reduction techniques. Two-step method consists of synthesis of nanoparticles and distribution of nanoparticles in carrier fluid. In the first stage, nanoparticles are synthesized using chemical or physical techniques such as chemical precipitation, sol-gel, sonochemical techniques, etc. The size and shape of the nano-sized particles could be regulated by adjusting the synthesis factors such as temperature, pH, and concentration of precursors. In the second stage, the synthesized nanoparticles are disseminated in a carrier fluid for instance H<sub>2</sub>O, thermic oil, or ethylene glycol (EG). The dispersion process is typically achieved by using a surfactant or a dispersant. The surfactant or dispersant prevents the nanoparticles from agglomerating and stabilizes the distribution. Suspended nano-sized particles in the carrier fluid are continuously stirred using mechanical stirrer or magnetic stirrer to disseminate the nano-sized particles in the fluid uniformly [5]. Furthermore, Bath sonication or probe sonication method is employed to improve nanofluid stability for long duration [6].

The two-step method of nanofluid synthesis has several advantages such as the ability to control the nanoparticle's shape and size, high stability of the resulting nanofluid, and low cost of production [7]. However, it also has some limitations such as the need for specialized equipment and the potential toxicity of the surfactants or dispersants used [8]. The stability of aluminum oxide (Al<sub>2</sub>O<sub>3</sub>) water nanofluid synthesized utilizing the two-step process and CTAB surfactant has been improved by researchers employing novel techniques. To promote long-term stability and avoid particle aggregation, these developments include optimizing the pH, mixing conditions, surfactant content, and dual sonication with simultaneous heating [8].

Joshi et al. [9] executed an experimental study with Al<sub>2</sub>O<sub>3</sub> nano-suspension in a vapor compression refrigeration system using two refrigerants, tetra-fluoro-ethane, and iso-butane. Authors used two-step technique for nanofluid synthesis. The study aimed to evaluate the effect of nano-synthesized fluids on the refrigeration system performance. Maximum COP (Coefficient of performance) enhancement of 41.9% was reported by researchers. Bindu and Herbert [10] developed multi-wall carbon nanotube, Al<sub>2</sub>O<sub>3</sub>, and ZnO (Zinc Oxide) nano-sized particles in aqua with two-step technique. Mono, binary and ternary nanofluid was synthesized to measure nanofluid stability and thermal conductivity. Researchers reported greater stability and thermal conductivity at higher bath temperatures during stirring and sonication process. Syarif et al. [11] used bath sonication technique to synthesize stable Al<sub>2</sub>O<sub>3</sub>-water nanofluid and reported better stability for more than three weeks. Singh et al. [12] synthesized aqua Al<sub>2</sub>O<sub>3</sub> nanofluid using CTAB (cetyltrimethylammonium bromide) surfactant. Synthesized nanofluid had shown better long-term stability and higher UV-absorbance value. Kanti et al. [13] used DLS and UV-spectrometry techniques to evaluate synthesized Al<sub>2</sub>O<sub>3</sub> nanofluid in ionic liquid with probe sonication. They had shown excellent stability for more than thirty days. Riahi et al. [14] used laser pulsation technique to synthesize stable Al<sub>2</sub>O<sub>3</sub>-water nanofluid. They used KD2Pro analyzer for thermal conductivity measurement of synthesized fluid. It was found to increase with volume fraction and temperature. Amalraj and Michael [15] synthesized Al<sub>2</sub>O<sub>3</sub> and CuO (Copper Oxide) nanofluids to investigate the performance of solar panels. Nanofluids had shown better performance in comparison with conventional fluids. Mehta and Subhedar [16] synthesized aqua Al<sub>2</sub>O<sub>3</sub> nanofluid using SDBS (Sodium Dodecyl Benzene Sulphonate) surfactant. Authors used two-step technique to synthesize stable nanofluid Thermo-physical properties have shown an incremental trend with rise in volume fraction of nanofluid. Dani et al. [17] performed study about the hydrothermal synthesis of aluminum oxide (Al<sub>2</sub>O<sub>3</sub>) nanoparticles to enhance the critical heat flux of nanofluids. The researchers used a

hydrothermal method to synthesize Al<sub>2</sub>O<sub>3</sub> nanoparticles with a mean diameter of 40–60 nm. They then dispersed the nanoparticles in water to create nanofluids and tested their heat transfer performance. The study suggests that the nanofluids with the Al<sub>2</sub>O<sub>3</sub> nanoparticles had an enhanced critical heat flux, which could be due to the increased thermal conductivity and surface area of the nano-sized particles. The study suggests that Al<sub>2</sub>O<sub>3</sub> nanoparticles synthesized through hydrothermal methods exhibit improvement in the heat transfer performance of nano-synthesized fluids.

Tiwari et al. [18] sonicated CeO<sub>2</sub> (Cerium dioxide)-MWCNT (Multi-wall Carbon Nanotube)/water nanofluid with CTAB surfactant. Authors reported improvement in stability and thermophysical properties of nanofluid due to attractive properties of CTAB surfactant. They preferred CTAB surfactant due to its cationic nature allows nanoparticles to attract more ions from surrounding base fluid ultimately resulting in development of electrical double layer and enhancement of repulsive force amongst consecutive nanoparticle molecules and developing stable nanofluid for longer time. Mostafizur et al. [19] synthesized Al<sub>2</sub>O<sub>3</sub>-Methanol nanofluid with CTAB surfactant to ensure long-term stability. Results reported stable nanofluid for more than one month with enhancement in nanofluid thermal conductivity and viscosity. Bahari et al. [20] used CTAB surfactant to synthesize aqua-based Al<sub>2</sub>O<sub>3</sub>-Silicon dioxide (SiO<sub>2</sub>) nanofluid.

Kanti et al. [21] synthesized mono and hybrid nanofluid using surfactant to examine effect of pH on stability and thermo-physical properties of nanofluid. Authors considered variation in volume fraction within 0.1% – 1% and reported pH as most influential parameter on thermal performance of nanofluid. Kanti et al. [22] synthesized Al<sub>2</sub>O<sub>3</sub> nanofluid to investigate effect of volume fraction and temperature on thermal conductivity. Authors reported augmentation in thermal conductivity with rise in volume concentration and temperature of nanofluid. Kanti et al. [23] used 1-ethyl-3-methylimidazolium chloride ionic base fluid to disperse Al<sub>2</sub>O<sub>3</sub> nanoparticles. Ionic nanofluid reported better long-term stability. Marulasiddeshi et al. [24] dispersed Al<sub>2</sub>O<sub>3</sub> and Al<sub>2</sub>O<sub>3</sub>-CuO (50:50) nanoparticles in water to investigate thermal conductivity of nanofluid. Authors reported higher thermal conductivity of hybrid nanofluid compared to mono nanofluid. Wanatasanappan et al. [25] used Al<sub>2</sub>O<sub>3</sub>:Fe<sub>2</sub>O<sub>3</sub> nanoparticles and water: Ethylene glycol base fluid to prepare stable nanofluid using two-step technique. Authors reported viscosity enhancement with particle volume fraction. Hybrid nanofluid showed Newtonian behavior.

Comparatively,  $\gamma$ -Al<sub>2</sub>O<sub>3</sub> nanoparticles have more surface area than  $\alpha$ -Al<sub>2</sub>O<sub>3</sub> nanoparticles [26]. Greater contact between the nanoparticles and the fluid medium is made possible by the increased surface area, which improves the dispersion and stability of the nanofluid. Additionally, the increased surface area offers more active locations for more heat interactions with surrounding fluid constituents which ultimately improves the heat transfer rate. Better dispersion throughout the fluid media is facilitated by  $\gamma$ -Al<sub>2</sub>O<sub>3</sub> owing to larger surface area and distinctive crystal structure.  $\gamma$ -Al<sub>2</sub>O<sub>3</sub> nanoparticles have a lower inclination to aggregate or settle and a higher tendency to distribute uniformly. The stability of the nanofluid must be maintained throughout time, which depends on this better dispersion leads to improve its suitability in different heat transfer applications [27].

Nanofluid with CTAB surfactant had shown better long-term stability and greater enhancement in thermal conductivity. CTAB has a positive charge since it is a cationic surfactant. SDS, in contrast, is a negatively charged anionic surfactant. However, negatively charged nanoparticles like Al<sub>2</sub>O<sub>3</sub> may respond better to the affinity and adsorption of positively charged surfactants like CTAB [20]. This may lead to better control over particle form and size as well as increased stability and dispersion of the nanoparticles in water. Nanoparticles can resist aggregation and sedimentation due to the CTAB's cationic properties, which can intensify electrostatic attraction between them. When long-term stability and resistance to settling or flocculation are sought, this greater stability can be especially helpful. The synthesized Al<sub>2</sub>O<sub>3</sub> nanoparticles may undergo

additional surface alterations or functionalization due to the cationic nature of CTAB surfactant. The introduction of particular features or functions to the surfaces of the nanoparticles is made possible by the surfactant's positive charge, which can allow interactions with negatively charged molecules. The thermal conductivity of the nanofluid may be improved by adding CTAB surfactant during the production process. To improve heat transport within the fluid and reduce interfacial thermal resistance, the surfactant molecules can form a thin layer around the nanoparticles [28].

The present research aims to synthesize stable gamma  $\text{Al}_2\text{O}_3$ -water nanofluid to investigate the thermal conductivity and dynamic viscosity of nanofluid. Two-step technique is used for synthesis of nanofluids. To enhance thermo-migration and Brownian diffusion effect, nanofluid was stirred at higher base temperature of  $60^\circ\text{C}$ . The present research adopts magnetic stirring with simultaneous heating which is followed by dual sonication process of bath sonication with simultaneous heating followed by probe sonication to intensify long-term stability. Experimental results of stability, thermal conductivity, and viscosity of aqua-based  $\text{Al}_2\text{O}_3$  nanofluid synthesized with CTAB surfactant are compared with that without surfactant to determine the influence of CTAB surfactant on enhancement of stability and thermophysical properties of nanofluids which makes it suitable for several thermal applications.

## 2. Material preparation

Aluminum Oxide ( $\gamma\text{-Al}_2\text{O}_3$ ) nanoparticles (Nanoshel, USA) having spherical shape with 20 nm mean nanoparticle diameter and 99.9% purity are used for nanofluid synthesis. Nanoparticles consist of  $3870\text{ kg/m}^3$  bulk density and conductivity of  $36\text{ W/m.K}$ . Fig. 1. (a) and (b) shows photograph of  $\gamma\text{-Al}_2\text{O}_3$  nanoparticles. Figs. 2 and 3 shows XRD result and SEM image of nanoparticles. XRD (D2phaser, Beauker, USA) is used to conduct experiment. The nano-powder is put on a glass slide and exposed to an X-ray beam to conduct XRD investigation on gamma  $\text{Al}_2\text{O}_3$  nanoparticles. The electrons in the sample's atoms cause the X-ray beam to scatter in various directions as it interacts with the sample's atoms. The intensity of the scattered X-rays is then calculated as a function of the scattering angle ( $2\theta$ ) after the scattered X-rays have been detected by a detector. Result shows sharp peak at  $25.41^\circ$ ,  $34.97^\circ$ ,  $43.17^\circ$ , and  $57.34^\circ$   $2\theta$  angle which confirms the  $\gamma$  phase of  $\text{Al}_2\text{O}_3$  nanoparticles [9].

SEM image of nano-powder is taken with the Scanning Electron Microscope (JEOL, USA). To perform SEM analysis, the  $\text{Al}_2\text{O}_3$  nanoparticles are first dispersed onto a conductive substrate, such as a carbon-coated copper grid. The sample is then placed into the SEM chamber and scanned with a focused beam of electrons. Result has shown spherical particle shape and an average particle size of less than 25 nm.

Deionized, distilled water is employed as carrier fluid. Carrier fluid of 200 ml volume is considered for synthesis of nanofluid. Nanoparticle

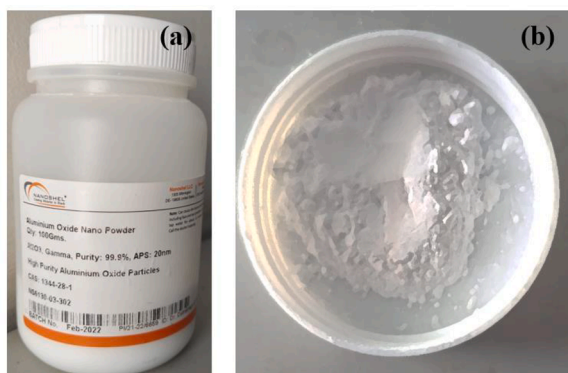


Fig. 1. Photograph of  $\gamma\text{-Al}_2\text{O}_3$  nanoparticles.

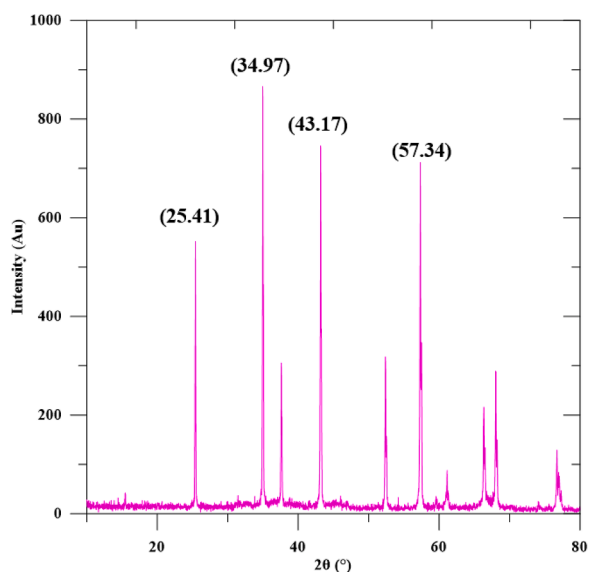


Fig. 2. X-ray diffraction results of  $\text{Al}_2\text{O}_3$  nano-powder.

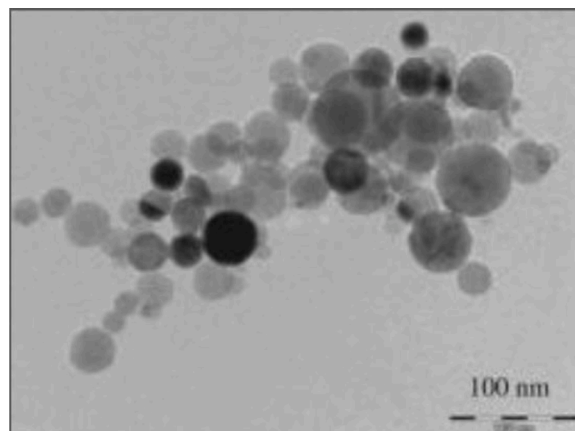


Fig. 3. SEM result of  $\text{Al}_2\text{O}_3$  nano-powder.

having several volume concentrations of 0.25%, 0.5%, 0.75%, and 1% is used for sample preparation. Eq. (i) shows relation between volume fraction, volume of the base fluid, and mass of the nanoparticles.

$$\varphi = \frac{\frac{m_{np}}{\rho_{np}}}{\frac{m_{np}}{\rho_{np}} + V_{bf}} \quad (i)$$

Whereas  $m_{np}$  is mass of nanoparticles,  $\rho_{np}$  is density of nanoparticles,  $V_{bf}$  is volume of carrier fluid and  $\varphi$  is volume concentration of nanoparticles. Mass of the nanoparticles is measured using setra balance unit. Unit consists of 0.001 gm accuracy during measurement of mass of the particles. CTAB surfactant (LOBA chemie) is used as cationic surfactant to enhance repulsive force between two consecutive molecules of nanoparticles which ultimately avoids agglomeration and sedimentation of nanoparticles and improves long-term stability. Mass of surfactant is considered as 33% of mass of the nanoparticles.

REMI (2 MLH) magnetic stirrer with hot plate is used for continuous stirring of nanofluid. Firstly, surfactant of prescribed mass is added to the prescribed volume of base fluid at constant speed of 500 RPM for 90 min. Then, prescribed mass of nanoparticles is added to the homogeneous solution and stirred for further 90 min by keeping base fluid temperature at  $60^\circ\text{C}$ . Higher base fluid temperature results in augmented thermo-migration and brownian diffusion effect results in better distribution of nano-sized particles in carrier fluid. After stirring

process, prepared fluid is sonicated by bath sonicator (M-5 US model, Samarth electronics pvt. Ltd., India) with simultaneous heating for an hour. Device consists of 200 W ultrasonic power capacity and 30 kHz frequency along with heating up to 60 °C fluid temperature. To further enhance stability, prepared fluid is sonicated using probe sonicator having model no. VC505 made by Sonics, USA. Sonicator consists of 500 W, 20 kHz specification. Nanofluid is sonicated using probe sonicator for 120 min and exhibits better particle dispersion and long-term stability. Magnetic stirring, bath sonication, and probe sonication technique is demonstrated in Fig. 4(a), (b), and (c). In case of synthesis of nanofluid without surfactant, nanoparticles are directly dispersed in the base fluid and synthesized by magnetic stirring, bath sonication, and probe sonication.

Table 1 shows the details of the instruments used in the experimentation.

### 3. Stability measurement techniques

Several techniques such as visual technique, UV-spectrometry, and DLS technique were used to evaluate stability of synthesized nanofluid and their results were discussed as follows.

#### 3.1. Visual technique

Visual technique is the simplest way to analyze stability of synthesized nanofluid. In this technique, synthesized fluid is kept steady in the container without giving any external agitation. Fluid sample is continuously observed for a specific time to observe sedimentation of nanoparticles. Severe sedimentation of nanoparticles results in color change of synthesized fluid and could be considered as unstable nanofluid. Fig 5. (a–d) shows photograph of synthesized fluid without CTAB surfactant having volume fraction ( $\phi = 1\%$ ) after 1 day, 8 days, 15 days, and 30 days from the day of synthesis of nanofluid. Similarly, Fig. 5. (e–h) depicts photograph of synthesized fluid with CTAB surfactant having volume fraction ( $\phi = 1\%$ ) after 1 day, 8 days, 15 days, and 30 days from the day of synthesis of nanofluid. Results demonstrate sedimentation of nanoparticles in the carrier fluid after 15 days from synthesis in case of nanofluid without CTAB surfactant, however, nanofluid with CTAB surfactant exhibits better long-term stability even after 30 days from the synthesis. CTAB surfactant consists of long H–C (hydrocarbon) molecular chain which makes it a good stabilizer and results in better long-term stability.

#### 3.2. UV-spectrometry

Shimadzu UV-1800 UV spectrometer is used to measure absorbance power of nanofluid after several intervals of time. It consists of source lamp release radiation waves having wavelength varying from 190 nm to 1100 nm with bandwidth of 1 nm. It consists of wavelength accuracy and reproducibility of  $\pm 0.1$  nm. The device consists of absorbance

capacity of up to 4 Au (Absorbance Unit). As per results shown in Fig. 6, Nanofluid with CTAB surfactant has shown higher absorbance compared to that without surfactant. Higher absorbance shows better dispersion of nanoparticles in the carrier fluid due to presence of CTAB surfactant, as it consists of positively charged molecules that interact with negatively charged nanoparticles and enhance repulsive force between consecutive nanoparticles and enhance fluid stability. CTAB molecules also consist of hydrophobic tail which is responsible for formation of electrical double layer and reduces agglomeration of nanoparticles. Highest absorbance of 2.68 Au is reported for highest volume fraction of nanofluid with CTAB surfactant. Higher absorbance shows higher nanoparticles suspended in the base fluid. Absorbance power was found to decrease with time proceeds for all samples. Sedimentation rate was found higher during initial days. Results show considerable stability of nanofluid after 30 days for all volume concentrations of nanofluids with surfactant.

Where NF is nanofluid, WS is with surfactant and WOS is without surfactant.

#### 3.3. Dynamic light scattering technique

DLS (Dynamic Light Scattering) technique measures mean nanoparticle size suspended in the nanofluid which ultimately shows the rate of agglomeration and stability of synthesized fluid. Particle size analyzer (Zetasizer, 7.13), Malvern Panalytical, is used to evaluate particle diameter of suspended nano-sized particles in the nanofluid. The device can measure particle size varying in the range from 3 nm to 100 nm and require 20  $\mu$ l sample size. Device consists of maximum uncertainty of  $\pm 3\%$ . Fig. 7(a) and (b) show results of nanofluid samples having 1% volume fraction without surfactant tested on Day 1 and Day 30 after synthesis of nanofluid. Results demonstrate larger mean particle size of 80 nm and 536 nm for the nanofluid samples without surfactant tested at Day 1 and Day 30 after nanofluid synthesis which depicts higher agglomeration and aggregation of nanoparticles in the carrier fluid results in poor stability. Fig. 7(c) and (d) show results of nanofluid sample having 1% volume fraction with surfactant tested on Day 1 and Day 30 after synthesis of nanofluid. Sample tested after day 1 has shown average particle size of 24 nm while the same on day 30 has shown average particle size of 54 nm. Results have shown better stability of nanofluid after 1 month. Better long-term stability is due to the presence of CTAB molecules which are being adsorbed by the surface of aluminum oxide nanoparticles and enhances repulsive force between consecutive molecules.

Where NF is nanofluid, WS is with surfactant and WOS is without surfactant.

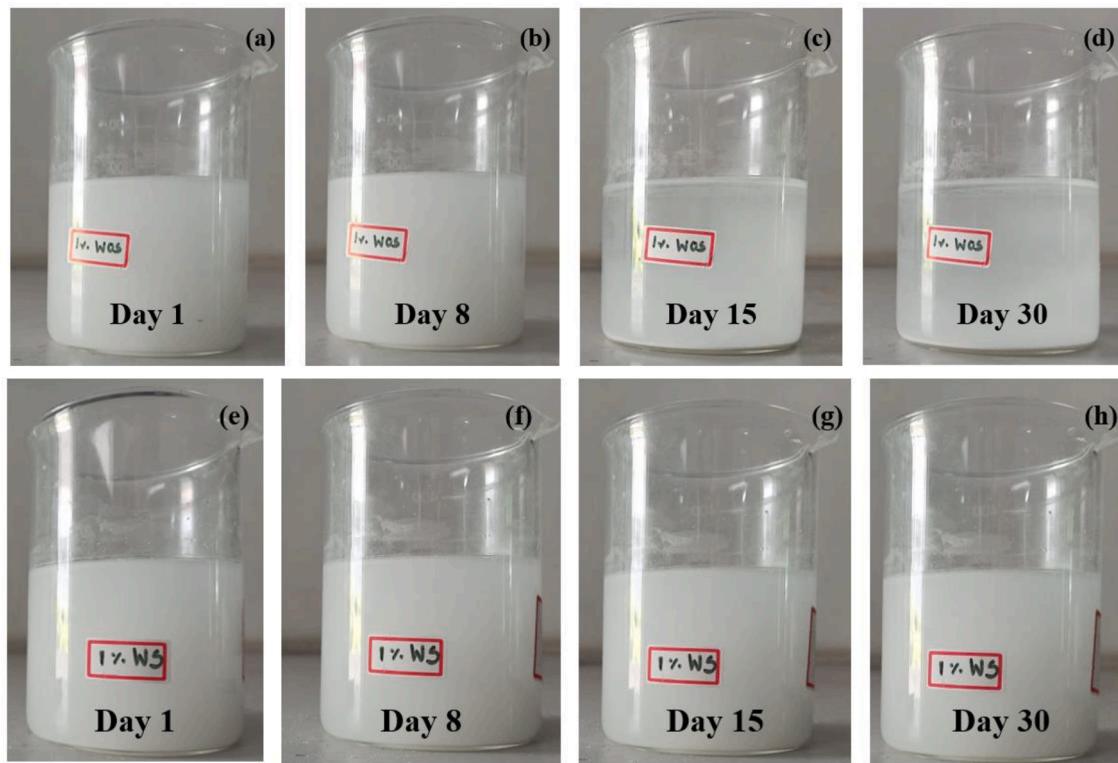
Fig. 8 shows the variation in average diameter of nanoparticles in nanofluids with various time intervals. Results also compare increment in particle size with time for various volume fraction nanofluids. Nanofluids without surfactant have shown greater rise in particle size with time in comparison with other nanofluid.



Fig. 4. (a) Magnetic stirring with heating (b) bath sonication with heating (c) Sonication with probe sonicator.

**Table 1**  
Instrumental details.

Instrument name	Measured parameter	Model no.	Manufacturer details	Range	Accuracy
Weighing balance	Nanoparticle mass	BL-200	Setra balance	0 – 200 g	±0.001 g
UV spectrometer	Absorbance Unit (Au)	UV-1800	Shimadzu, USA	–4 – 4 Au	±0.01 Au
Particle size analyzer	Mean size of suspended particles	Zetasizer, 7.13	Malvern Panalytical, UK	3 – 100 nm	±0.3 nm
KD2Pro thermal analyzer	Thermal Conductivity	TEMPOS	Decagon Devices, USA	0.02 – 2 W/m. K	±0.0004 W/m. K
Viscometer	Dynamic Viscosity	MCR-301	Anton Paar, Austria	0.0004 – 0.05 N.s/m <sup>2</sup>	±0.00001 N.s/m <sup>2</sup>



**Fig. 5.** (a–d) Photographs of visual inspection of aqua  $\text{Al}_2\text{O}_3$  nanofluid without CTAB surfactant; (e–h) Photographs of visual inspection of aqua  $\text{Al}_2\text{O}_3$  nanofluid with CTAB surfactant.

#### 4. Thermophysical properties of nanofluids

In this section, thermal conductivity and viscosity of nanofluids with various volume fractions were measured. Experiments were performed after 30 days from the day at which nanofluid samples were prepared. All the experiments were repeated three times and mean of three results was considered for analysis. Thermophysical properties of various samples are measured at 25 °C temperature. Results were compared with standard mathematical products for validation. Effect of temperature variation on thermophysical properties of nanofluids was examined during the experimentation.

To test the thermal conductivity of a nanofluid, a KD2Pro thermal analyzer, Decagon Devices, USA with a KS 1 sensor is employed. Nanofluid is filled in 15 ml container and KS 1 sensor is inserted in the sample. Tube is fixed in the fixture to avoid unnecessary disturbance during measurement. Device can measure the thermal conductivity of nanofluid in the range of 0.02 – 2 W/m. K with uncertainty of ±2%. Thermal conductivity of Nanofluid with and without surfactant was measured and found to increase with nanoparticle's volume concentration. Possible reasons for augmentation in nanofluid thermal conductivity are higher nanoparticles thermal conductivity, larger surface area between fluid and solid particles, continuous molecular movement of nanoparticles, and particle movement due to temperature gradient within synthesized fluid [2,6–7]. Nanofluid with CTAB surfactant

demonstrated higher thermal conductivity in comparison with fluid without surfactant. CTAB surfactant due to its lower thermal conductivity lowers thermal conductivity of synthesized fluid, however, CTAB surfactant improves stability of synthesized fluid and restricts particle agglomeration and sedimentation exhibits greater brownian diffusion and thermo-migration effect which ultimately improves thermal conductivity of synthesized fluid. Enhancement in thermal conductivity of nanofluid with surfactant at several volume fractions as with 0.25%, 0.5%, 0.75%, and 1% was 1.9%, 3.9%, 6.4%, and 8.5%, while, 1.3%, 3.2%, 5.5%, and 6.7% for fluid without surfactant respectively in comparison with base fluid. Change in nanofluid thermal conductivity with volume concentration is represented in Fig. 9. Said et al. [29], Esfe et al. [30], Sundar et al. [31], and Subhedar et al. [32] reported augmentation in thermal conductivity with nanofluid volume fraction.

Results received from experimentation are compared with Hamilton and Crosser [33] and xue model [34] depicted by Eqs (ii) and (iii) respectively. Deviation in experimental results and predicted results were found to increase with increase in volume fraction. Maximum deviation reported is 4.2% at highest volume fraction (1%). As theoretical models could not be able to predict effect of nanoparticle diffusion in synthesized fluid which is accountable for thermal conductivity augmentation of nanofluid.

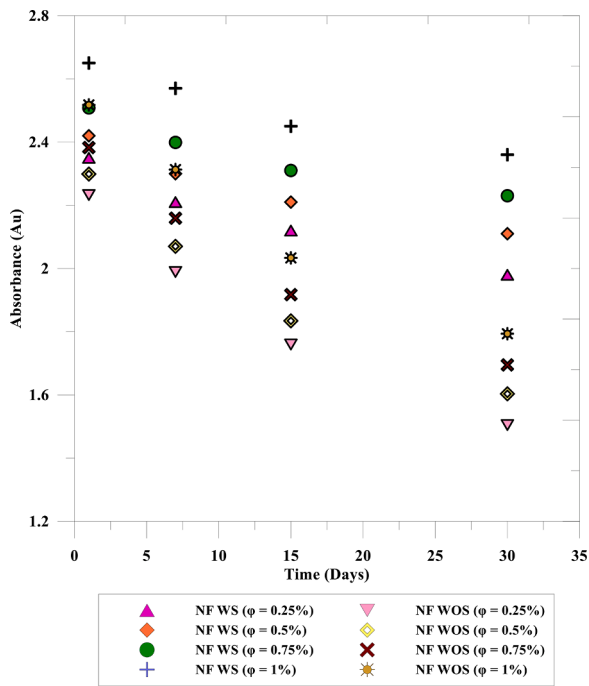


Fig. 6. UV-spectrometry result.

$$\frac{k_{nf}}{k_{bf}} = \frac{k_{np} + (n - 1)k_{bf} - (n - 1)\varphi(k_{bf} - k_{np})}{(n - 1)k_{bf} + k_{np} + \varphi(k_{bf} - k_{np})} \quad (ii)$$

$$\frac{k_{nf}}{k_{bf}} = \frac{1 - \varphi + 2\varphi \frac{k_{np}}{(k_{np} - k_{bf})} \log_e \left( \frac{k_{np} + k_{bf}}{(2k_{bf})} \right)}{1 - \varphi + 2\varphi \frac{k_{bf}}{(k_{np} - k_{bf})} \log_e \left( \frac{k_{np} + k_{bf}}{(2k_{bf})} \right)} \quad (iii)$$

Where  $k_{nf}$  is nanofluid thermal conductivity,  $k_{bf}$  is base fluid thermal conductivity,  $k_{np}$  is nanoparticle thermal conductivity,  $n = 3/\psi$ , where,  $\psi$  is particle sphericity and  $\varphi$  is volume concentration of nanofluid.

From the experimental results, following correlation was developed to determine thermal conductivity ratio ( $k_{nf}/k_{bf}$ ) for a given volume fraction.

$$\frac{k_{nf}}{k_{bf}} = 1 + 15.469\varphi \quad (iv)$$

Fig. 10 shows variation in thermal conductivity of nanofluid with temperature for different volume fractions of nanoparticles in synthesized nanofluid with surfactant. Temperature of fluid was varied from 25 °C to 65 °C using the water bath (RSB-12), Janki Impex pvt. Ltd., India. Device consists of temperature accuracy of  $\pm 0.1$  °C. Sample was allowed to submerge in the bath for 10 min before measurement to achieve steady state condition. Result shows increase in thermal conductivity of nanofluid with temperature for all the samples. Increasing trend of thermal conductivity with temperature could be justified by intense brownian diffusion effect and thermos-migration effect at elevated temperatures and decrease in thermal boundary resistance between nanoparticles and surrounding fluid at elevated temperatures. Maximum enhancement in thermal conductivity was reported as 16.8% for 1% volume concentration at 65 °C compared to fluid with same concentration at 25 °C. Moldoveanu et al. [35] reported augmentation in nanofluid thermal conductivity with nanofluid temperature rise. Similar trends were reported by Kumar et al. [36], Abdolbaqi et al. [37], and Mukherjee et al. [38].

Anton Paar rotating cylinder type viscometer is being used for measurement of dynamic viscosity of nanofluid. Maximum sample size for viscosity measurement is 5  $\mu$ l. Device can operate with temperature

range of  $-10$  °C –  $80$  °C. Instrument can measure the data with  $\pm 1\%$  accuracy. Fig. 11 shows change in nanofluid viscosity with volume fraction of nanoparticles. Experimentation includes comparison of the viscosity of nanofluid with and without surfactant with that of carrier fluid. Base fluid reported lowest dynamic viscosity and by adding nanoparticles, dynamic viscosity was found to increase with volume fraction. Gain in dynamic viscosity followed exponential trend. Presence of nanoparticles in base fluid forms relative motion between liquid and solid particles creating resistance force found responsible for viscosity rise. Furthermore, brownian diffusion movement of nanoparticles forms eddies in surrounding fluid and enhances resistance force. In continuation, nanoparticles due to van der Waal’s force cause particle cluster formation resulting in viscosity enhancement [39–41]. Experimental results are compared with theoretical models developed by Williams [42], Tseng and Ling [43], and Brinkman [44] shown by Eqs (v), (vi), and (vii). Model developed by Tseng and Ling was from experimental results performed for similar volume fraction range.

Addition of surfactant in nanofluid reported higher viscosity in comparison with fluid without surfactant. The reason may be due to the coating of surfactant molecules on nanoparticles leads to increase in particle size causing a rise in resistance force and viscosity, Furthermore, addition of surfactant in carrier fluid influences its molecular structure and intern molecular forces which ultimately increase viscosity [45]. At 1% volume fraction, viscosity of nanofluid with surfactant was found 16% higher as compared to that without surfactant. Maximum enhancement reported by nanofluid with 1% volume fraction with surfactant was 76.2%.

$$\frac{\mu_{nf}}{\mu_{bf}} = e^{\left[ \frac{4.91\varphi}{(0.2092-\varphi)} \right]} \quad (v)$$

$$\frac{\mu_{nf}}{\mu_{bf}} = 13.47e^{35.98\varphi} \quad (vi)$$

$$\frac{\mu_{nf}}{\mu_{bf}} = \frac{1}{(1 - \varphi)^{2.5}} \quad (vii)$$

From the experimental results, following correlation was proposed to predict viscosity ratio ( $\mu_{nf}/\mu_{bf}$ ) with volume fraction.

$$\frac{\mu_{nf}}{\mu_{bf}} = 1.074e^{84.463\varphi} \quad (v)$$

Variation in dynamic viscosity of nanofluid with temperature is shown in Fig. 12. Temperature of the synthesized fluid was varied from 25 °C to 65 °C. Viscosity was found to decrease with rise in temperature for all the samples of nanofluid with surfactant. The reason may be due to base fluid’s viscosity typically decreases as a nanofluid temperature rises because the intermolecular connections between the fluid molecules become weaker. The total viscosity of the nanofluid may also decrease as a result of this decrease in the viscosity of the base fluid. The thermal energy of the nanoparticles rises at higher temperatures, increasing their Brownian motion. The effective size and concentration of the nanoparticle clusters may diminish as a result of the nanoparticles moving more freely and independently. The effective viscosity of the nanofluid may decrease as the concentration and size of the nanoparticle clusters decline. For 1% volume fraction, viscosity was found to decrease by 30.7%, when fluid temperature was raised from 25 °C to 65 °C. Marulasiddeshi et al. [24], Wanatasanappan et al. [25], and Subhedar et al. [32] reported similar trend of increase and decrease in viscosity with Volume fraction and temperature of nanofluid.

## 5. Conclusion

This research aims at the synthesis of  $Al_2O_3$ -water nanofluid having long-term stability. Influence of CTAB surfactant on long-term stability and thermo-physical properties was evaluated. Two-step method was

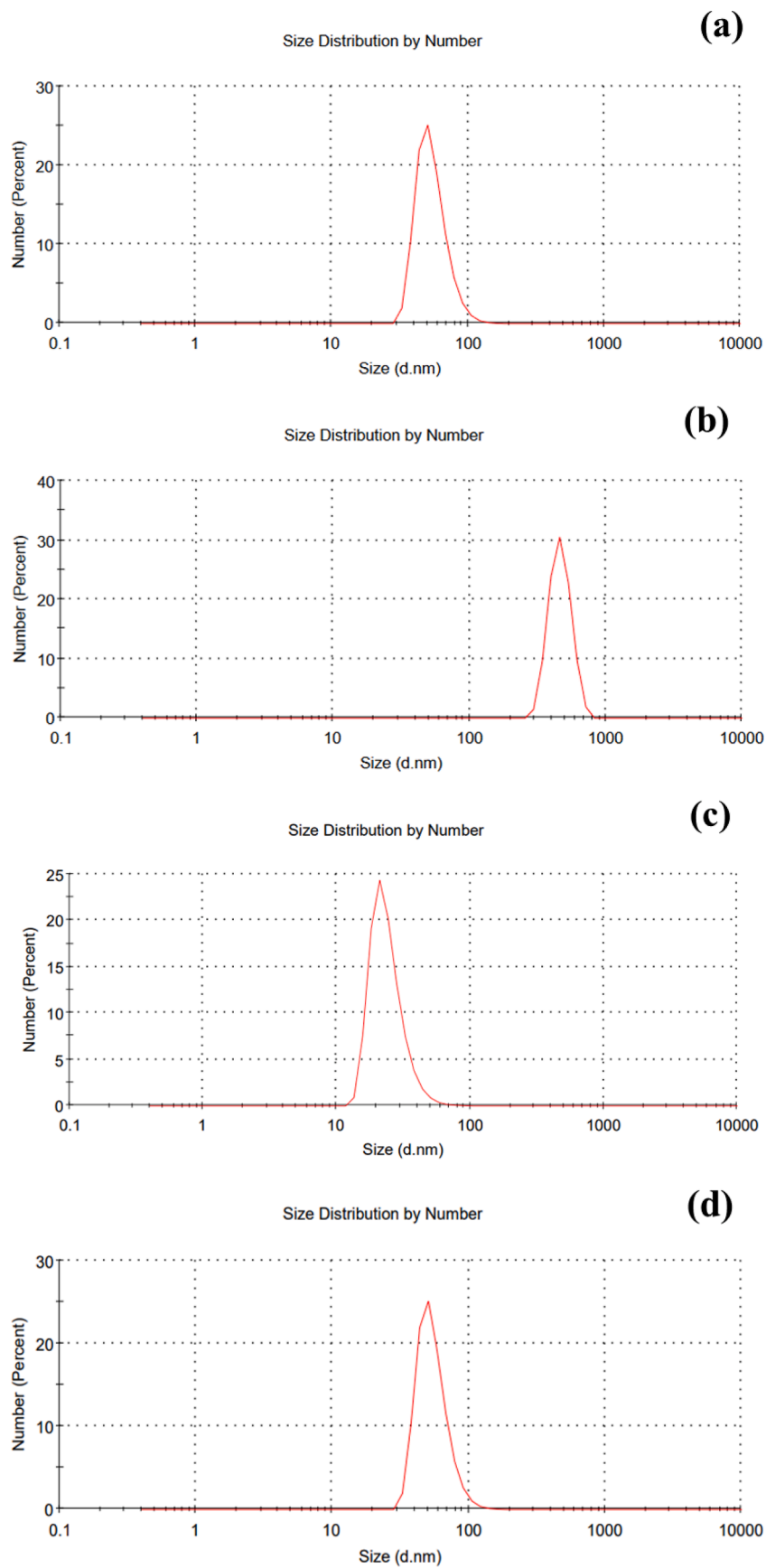


Fig. 7. DLS results of nanofluids (a) NF WOS ( $\varphi = 1\%$ ) at Day 1, (b) NF WOS ( $\varphi = 1\%$ ) at Day 30 (c) NF WS ( $\varphi = 1\%$ ) at Day 1, (d) NF WS ( $\varphi = 1\%$ ) at day 30.

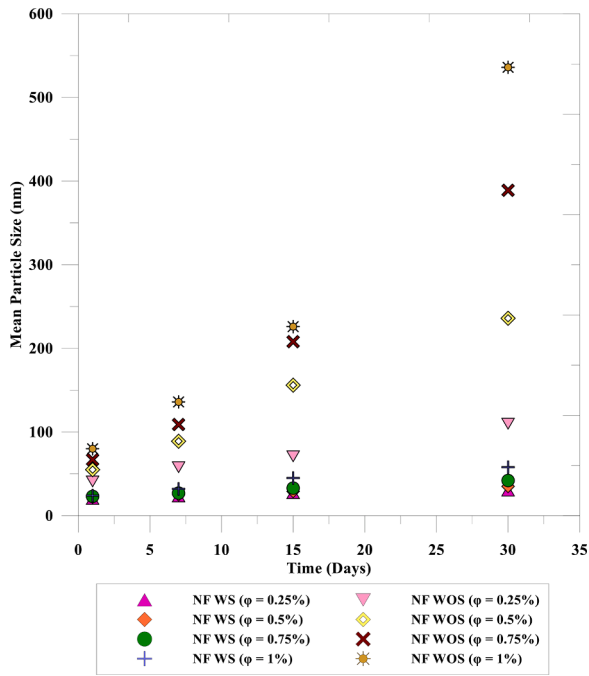


Fig. 8. DLS results for various samples.

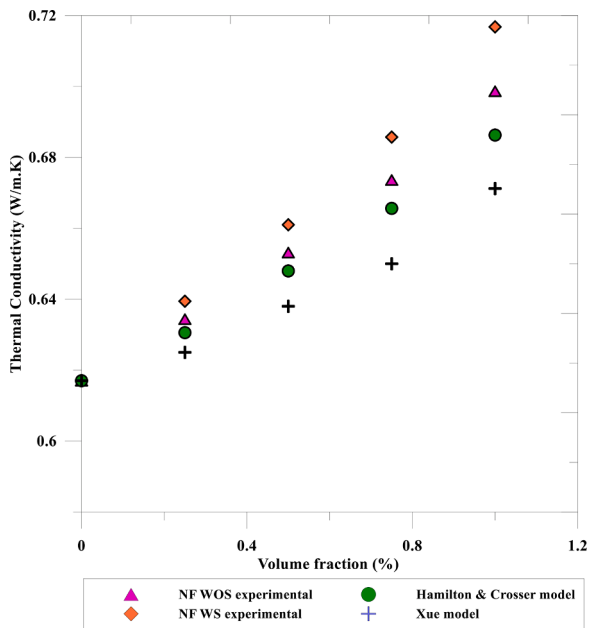


Fig. 9. Variation of nanofluid thermal conductivity with volume fraction.

employed to synthesize nanofluid having several volume concentrations in the range of 0.25%–1%. Magnetic stirring with simultaneous heating followed by dual sonication (Bath sonication with heating, and probe sonication process) is used to improve long-term stability. Synthesized nanofluids were characterized by particle size analyzer, UV-spectrometer, KD2Pro analyzer, and viscometer. Following points were concluded from the experimental study.

- Use of cationic Cetyltrimethylammonium bromide (CTAB) surfactant, Magnetic stirring with simultaneous heating followed by dual sonication improves nanofluid stability for a longer duration.
- Visual inspection technique has clearly shown better long-term stability for nanofluid synthesized with CTAB surfactant. Results were

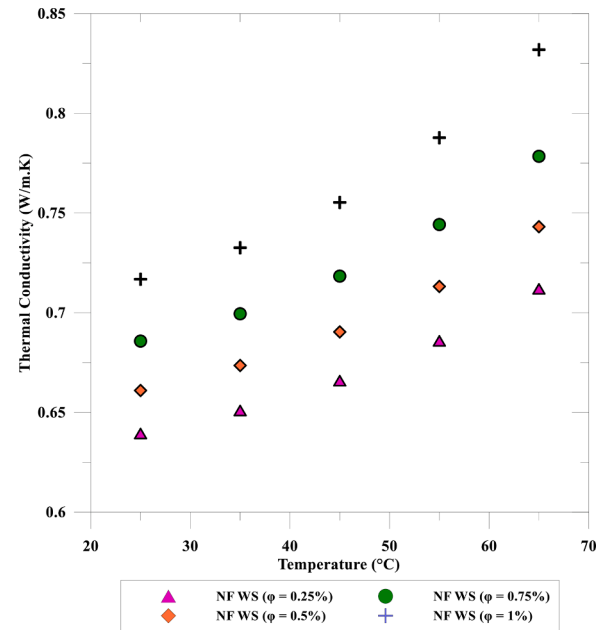


Fig. 10. Variation in nanofluid thermal conductivity with temperature.

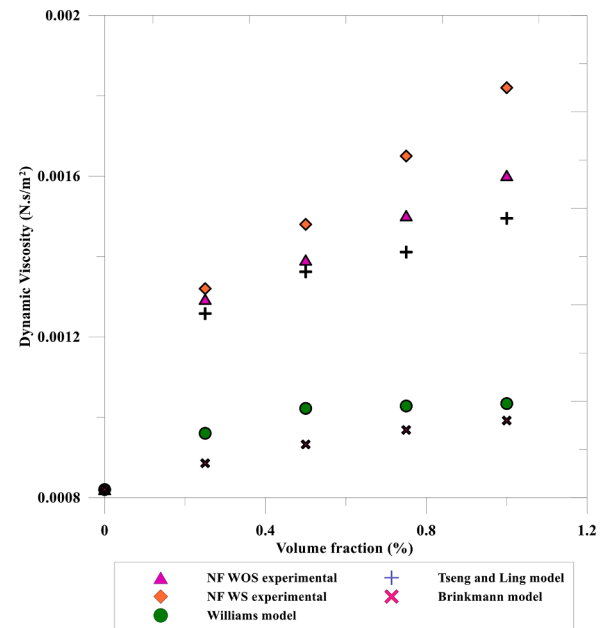


Fig. 11. Variation in nanofluid dynamic viscosity with volume fraction.

supported by DLS technique which has described highest particle size of 80 nm and 534 nm for nanofluid with and without surfactant respectively with 1% volume fraction on 30th day from synthesis which shows heavy particle agglomeration for the sample without surfactant. UV results have shown gradual decrement in absorbance (Au) with time for both the samples, however, rate of decrement in absorbance of nanofluid with surfactant is relatively lower than that without surfactant.

- Thermal conductivity and viscosity of nanofluid were found to increase with rise in nanoparticle's volume fraction in base fluid. Rise in thermal conductivity has followed linear trend while viscosity rise has shown exponential trend. Thermal conductivity and viscosity of nanofluid were found higher for samples with surfactant compared to that without surfactant. Maximum enhancement in thermal



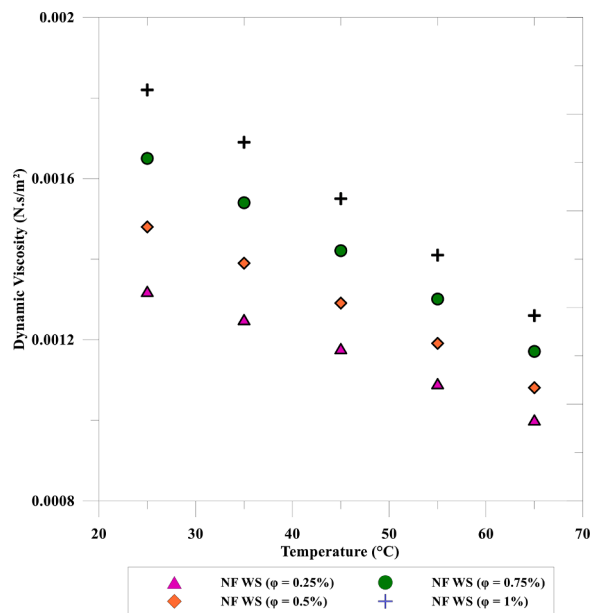


Fig. 12. Variation in nanofluid dynamic viscosity with temperature.

conductivity and viscosity of nanofluid was found to be 8.5% and 76.2% respectively at highest volume fraction for fluid with surfactant.

- Thermal conductivity was found to be increasing with temperature showing maximum enhancement of 16.8% for 1% volume fraction and 65°C temperature, nevertheless, viscosity has shown decrement with temperature rise with maximum drop of 30.7% for the similar working condition.
- Effect of variation in CTAB concentration in synthesized nanofluid on its stability and thermo-physical properties could be evaluated. Suitability of CTAB surfactant with other thermic fluids and nanoparticles needs to be investigated.

#### Declaration of Competing Interest

We have no conflict of interest

#### Data availability

Data will be made available on request.

#### Acknowledgement

This work was supported by Qatar National Research Fund under the grant no. MME03-1226-210042. The statements made herein are solely the responsibility of the authors. Authors are also thankful to Charotar University of Science & Technology, Changa for allowing to use their resources.

#### Supplementary materials

Supplementary material associated with this article can be found, in the online version, at [doi:10.1016/j.ijft.2023.100410](https://doi.org/10.1016/j.ijft.2023.100410).

#### References

- [1] M. Elkelay, E.A. El Shenawy, H. Alm-Eldin Bastawissi, M.M. Shams, H. Panchal, A comprehensive review on the effects of diesel/biofuel blends with nanofluid additives on compression ignition engine by response surface methodology, *Energy Convers. Manag.* X 14 (2022). Article 100177.

- [2] H. Panchal, H. Nurdianto, K.K. Sadasivuni, S.S. Hishan, F.A. Essa, M. Khalid, S. Dharaskar, S. Shanmugan, Experimental investigation on the yield of solar still using manganese oxide nanoparticles coated absorber, *Case Stud. Therm. Eng.* 25 (2021). Article 100905.
- [3] B. Mehta, D. Subhedar, H. Panchal, Z. Said, Synthesis, stability, thermophysical properties and heat transfer applications of nanofluid—a review, *J. Mol. Liq.* (2022), 120034. Aug 6.
- [4] M. Vaka, R. Walvekar, A.K. Rasheed, M. Khalid, H. Panchal, A review: emphasizing the nanofluids use in PV/T systems, *IEEE Access* 8 (2020) 58227–58249, <https://doi.org/10.1109/ACCESS.2019.2950384>.
- [5] G.F. Smaism, D.B. Mohammed, A.M. Abdulhadi, K.F. Uktamov, F.H. Alsutany, S. E. Izzat, M.J. Ansari, H.H. Kzar, M.E. Al-Gazally, E. Kianfar, Nanofluids: properties and applications, *J. Solgel Sci. Technol.* 104 (1) (2022) 1–35. Oct.
- [6] Z. Said, S. Arora, S. Farooq, L.S. Sundar, C. Li, A. Allouhi, Recent advances on improved optical, thermal, and radiative characteristics of plasmonic nanofluids: academic insights and perspectives, *Sol. Energy Mater. Sol. Cells* 236 (2022), 111504. Mar 1.
- [7] B. Mehta, D. Subhedar, Review on mechanism and parameters affecting thermal conductivity of nanofluid, *Mater. Today: Proceedings* 56 (2022) 2031–2037. Jan 1.
- [8] Kumar L., Walvekar R., Khalid M. An overview of recent advancements and applications of hybrid nanofluids. *Mater. Today: Proceedings*. 2023 Feb 16.
- [9] Y.G. Joshi, D.R. Zanwar, S.S. Joshi, N.A. Bhave, Experimental investigation of Al<sub>2</sub>O<sub>3</sub> nanosuspension in vapor compression refrigeration system using tetrafluoroethane and iso-butane refrigerants, *Mater. Today: Proceedings* 50 (2022) 1804–1813. Jan 1.
- [10] M.V. Bindu, G.J. Herbert, Experimental investigation of stability, optical property and thermal conductivity of water based MWCNT-Al<sub>2</sub>O<sub>3</sub>-ZnO mono, binary and ternary nanofluid, *Synth. Met.* 287 (2022), 117058. Jul 1.
- [11] D.G. Syarif, H. Aliah, A.M. Efendi, H. Wafda, M. Yamin, D. Muliawan, Nanofluid of Al<sub>2</sub>O<sub>3</sub> and its response to gamma radiation, In: *AIP Conference Proceedings*, AIP Publishing LLC, 2022, 050008. Nov 14Vol. 2652, No. 1.
- [12] V. Singh, A. Kumar, M. Alam, A. Kumar, P. Kumar, V. Goyat, A study of morphology, UV measurements and zeta potential of zinc ferrite and Al<sub>2</sub>O<sub>3</sub> nanofluids, *Mater. Today: Proceedings* 59 (2022) 1034–1039. Jan 1.
- [13] P.K. Kanti, K.V. Sharma, A.R. HN, M. Karbasi, Z. Said, Experimental investigation of synthesized Al<sub>2</sub>O<sub>3</sub> Ionanofluid's energy storage properties: model-prediction using gene expression programming, *J. Energy Storage* 55 (2022), 105718. Nov 25.
- [14] A. Riahi, S. Khamlich, M. Balghouthi, T. Khamliche, T.B. Doyle, W. Dimassi, A. Guizani, M. Maaza, Study of thermal conductivity of synthesized Al<sub>2</sub>O<sub>3</sub>-water nanofluid by pulsed laser ablation in liquid, *J. Mol. Liq.* 304 (2020), 112694. Apr 15.
- [15] S. Amalraj, P.A. Michael, Synthesis and characterization of Al<sub>2</sub>O<sub>3</sub> and CuO nanoparticles into nanofluids for solar panel applications, *Results Phys.* 15 (2019), 102797. Dec 1.
- [16] B. Mehta, D. Subhedar, Synthesis and characterization of γ-Al<sub>2</sub>O<sub>3</sub>-Water nanofluid with and without surfactant, *Mater. Today: Proceedings* 62 (2022) 418–425. Jan 1.
- [17] G.S. Dani, H.P. Djoko, S.P. Jupiter, Hydrothermally synthesis of Al<sub>2</sub>O<sub>3</sub> nanoparticles for nanofluids with enhanced critical heat flux, in: *In Journal of Physics: Conference Series*, IOP Publishing, 2020, 012023. Vol. 1428, No. 1.
- [18] A.K. Tiwari, N.S. Pandya, Z. Said, H.F. Öztop, Abu-Hamdeh N. 4S consideration (synthesis, sonication, surfactant, stability) for the thermal conductivity of CeO<sub>2</sub> with MWCNT and water based hybrid nanofluid: an experimental assessment, *Colloids Surf. A: Physicochem. Eng. Aspects* 610 (2021), 125918. Feb 5.
- [19] R.M. Mostafizur, M.G. Rasul, M.N. Nabi, Effect of surfactant on stability, thermal conductivity, and viscosity of aluminium oxide–methanol nanofluids for heat transfer applications, *Therm. Sci. Eng. Prog.* 31 (2022), 101302. Jun 1.
- [20] N.M. Bahari, S.N. Che Mohamed Hussein, N.H. Othman, Synthesis of Al<sub>2</sub>O<sub>3</sub>-SiO<sub>2</sub>/water hybrid nanofluids and effects of surfactant toward dispersion and stability, *Part. Sci. Technol.* 39 (7) (2021) 844–858. Oct 3.
- [21] P.K. Kanti, P. Sharma, K.V. Sharma, M.P. Maiya, The effect of pH on stability and thermal performance of graphene oxide and copper oxide hybrid nanofluids for heat transfer applications: application of novel machine learning technique, *J. Energy Chem.* 82 (2023) 359–374. Jul 1.
- [22] P.K. Kanti, P. Sharma, M.P. Maiya, K.V. Sharma, The stability and thermophysical properties of Al<sub>2</sub>O<sub>3</sub>-graphene oxide hybrid nanofluids for solar energy applications: application of robust autoregressive modern machine learning technique, *Solar Energy Mater. Solar Cells* 253 (2023), 112207. May 1.
- [23] P.K. Kanti, E.I. Chereches, A.A. Minea, K.V. Sharma, Experiments on thermal properties of ionic liquid enhanced with alumina nanoparticles for solar applications, *J. Therm. Anal. Calorim.* (2022) 1–2. Aug 30.
- [24] H.B. Marulasiddeshi, P.K. Kanti, M. Jamei, S.B. Prakash, S.N. Sridhara, Z. Said, Experimental study on the thermal properties of Al<sub>2</sub>O<sub>3</sub>-CuO/water hybrid nanofluids: development of an artificial intelligence model, *Int. J. Energy Res.* 46 (15) (2022) 21066–21083. Dec.
- [25] V.V. Wanatasanappan, P.K. Kanti, P. Sharma, N. Husna, M.Z. Abdullah, Viscosity and rheological behavior of Al<sub>2</sub>O<sub>3</sub>-Fe<sub>2</sub>O<sub>3</sub>/water-EG based hybrid nanofluid: a new correlation based on mixture ratio, *J. Mol. Liq.* 375 (2023), 121365. Apr 1.
- [26] X. Zhou, Y. Wang, K. Zheng, H. Huang, Comparison of heat transfer performance of ZnO-PG, α-Al<sub>2</sub>O<sub>3</sub>-PG, and γ-Al<sub>2</sub>O<sub>3</sub>-PG nanofluids in car radiator, *Nanomater. Nanotechnol.* 9 (2019), 1847980419876465. Sep 16.
- [27] A. Akbarzadeh, M. Ahmadlouydarab, A. Niaei, Capabilities of α-Al<sub>2</sub>O<sub>3</sub>, γ-Al<sub>2</sub>O<sub>3</sub>, and bentonite dry powders used in flat plate solar collector for thermal energy storage, *Renew. Energy* 173 (2021) 704–720. Aug 1.
- [28] G. Xia, H. Jiang, R. Liu, Y. Zhai, Effects of surfactant on the stability and thermal conductivity of Al<sub>2</sub>O<sub>3</sub>/de-ionized water nanofluids, *Int. J. Therm. Sci.* 84 (2014) 118–124. Oct 1.

- [29] Z. Said, R. Saidur, A. Hepbasli, N.A. Rahim, New thermophysical properties of water based TiO<sub>2</sub> nanofluid—the hysteresis phenomenon revisited, *Int. Commun. Heat Mass Transf.* 58 (2014) 85–95. Nov 1.
- [30] M.H. Esfe, S. Saedodin, M. Mahmoudi, Experimental studies on the convective heat transfer performance and thermophysical properties of MgO–water nanofluid under turbulent flow, *Exp. Therm. Fluid Sci.* 52 (2014) 68–78. Jan 1.
- [31] L.S. Sundar, M.J. Hortiguera, M.K. Singh, A.C. Sousa, Thermal conductivity and viscosity of water based nanodiamond (ND) nanofluids: an experimental study, *Int. Commun. Heat Mass Transf.* 76 (2016) 245–255. Aug 1.
- [32] D.G. Subhedar, B.M. Ramani, K.V. Chauhan, H. Panchal, S.M. Prajapati, A.J. Al-rubaie, M.M. Jaber, Experimental study on the variation of car radiator frontal area using Al<sub>2</sub>O<sub>3</sub>/water-ethylene glycol nano coolant, *Proc. Inst. Mech. Eng., Part E: J. Process Mech. Eng.* (2023). Mar 209544089231159994.
- [33] R.L. Hamilton, O.K. Crosser, Thermal conductivity of heterogeneous two-component systems, *Ind. Eng. Chem. Fundamentals* 1 (3) (1962) 187–191. Aug.
- [34] Q.Z. Xue, Model for thermal conductivity of carbon nanotube-based composites, *Phys. B: Condens. Matter* 368 (1–4) (2005) 302–307. Nov 1.
- [35] G.M. Moldoveanu, G. Humnic, A.A. Minea, A. Humnic, Experimental study on thermal conductivity of stabilized Al<sub>2</sub>O<sub>3</sub> and SiO<sub>2</sub> nanofluids and their hybrid, *Int. J. Heat Mass Transf.* 127 (2018) 450–457. Dec 1.
- [36] N. Kumar, S.S. Sonawane, S.H. Sonawane, Experimental study of thermal conductivity, heat transfer and friction factor of Al<sub>2</sub>O<sub>3</sub> based nanofluid, *Int. Commun. Heat Mass Transf.* 90 (2018) 1. Jan 1-0.
- [37] M.K. Abdolbaqi, W.H. Azmi, R. Mamat, K.V. Sharma, G. Najafi, Experimental investigation of thermal conductivity and electrical conductivity of BioGlycol–water mixture based Al<sub>2</sub>O<sub>3</sub> nanofluid, *Appl. Therm. Eng.* 102 (2016) 932–941. Jun 5.
- [38] S. Mukherjee, P.C. Mishra, P. Chaudhuri, Thermo-economic performance analysis of Al<sub>2</sub>O<sub>3</sub>-water nanofluids—An experimental investigation, *J. Mol. Liq.* 299 (2020), 112200. Feb 1.
- [39] C. Ezekwem, A recent review of viscosity models for nanofluids, *Energy Sources, Part A: Recovery, Util. Environ. Effects* 44 (1) (2022) 1250–1315. Mar 31.
- [40] M. Klazly, G. Bognár, A novel empirical equation for the effective viscosity of nanofluids based on theoretical and empirical results, *Int. Commun. Heat Mass Transf.* 135 (2022), 106054. Jun 1.
- [41] M.M. Maseer, F.B. Alnaimi, R.M. Hannun, L.C. Wai, K.A. Al-Gburi, S.O. Mezan, A review of the characters of nanofluids used in the cooling of a photovoltaic-thermal collector, *Mater. Today: Proceedings* 57 (2022) 329–336. Jan 1.
- [42] W. Williams, J. Buongiorno, L.W. Hu, Experimental investigation of turbulent convective heat transfer and pressure loss of alumina/water and zirconia/water nanoparticle colloids (nanofluids) in horizontal tubes, *J. Heat Transfer* 130 (4) (2008). Apr 1.
- [43] W.J. Tseng, K.C. Lin, Rheology and colloidal structure of aqueous TiO<sub>2</sub> nanoparticle suspensions, *Mater. Sci. Eng.: A* 355 (1–2) (2003) 186–192. Aug 25.
- [44] H.C. Brinkman, The viscosity of concentrated suspensions and solutions, *J. Chem. Phys.* 20 (4) (1952) 571. Apr.
- [45] M. Awais, N. Ullah, J. Ahmad, F. Sikandar, M.M. Ehsan, S. Salehin, A.A. Bhuiyan, Heat transfer and pressure drop performance of nanofluid: a state-of-the-art review, *Int. J. Thermo fluids* 9 (2021), 100065. Feb 1.